

Environmental Science Atmospheres

Accepted Manuscript

This article can be cited before page numbers have been issued, to do this please use: H. Hata, Y. Nakamura, J. Vazquez Santiago and K. Tonokura, *Environ. Sci.: Atmos.*, 2025, DOI: 10.1039/D4EA00137K.



This is an Accepted Manuscript, which has been through the Royal Society of Chemistry peer review process and has been accepted for publication.

Accepted Manuscripts are published online shortly after acceptance, before technical editing, formatting and proof reading. Using this free service, authors can make their results available to the community, in citable form, before we publish the edited article. We will replace this Accepted Manuscript with the edited and formatted Advance Article as soon as it is available.

You can find more information about Accepted Manuscripts in the [Information for Authors](#).

Please note that technical editing may introduce minor changes to the text and/or graphics, which may alter content. The journal's standard [Terms & Conditions](#) and the [Ethical guidelines](#) still apply. In no event shall the Royal Society of Chemistry be held responsible for any errors or omissions in this Accepted Manuscript or any consequences arising from the use of any information it contains.

Atmospheric aerosols pose health risks to humans and animals and are also recognised as climate forcers. Therefore, understanding the fundamental chemistry of aerosol formation is crucial for the scientific community to address these issues. Criegee intermediates (CIs) are known precursors of sulphate and other atmospheric aerosols. While numerous studies have clarified the role of stabilised Criegee intermediates (sCIs) in aerosol formation, the impact of vibrationally-excited Criegee intermediates (vCIs), which produce OH radicals through unimolecular decomposition, has been less explored. This study quantifies the significance of vCIs in aerosol formation and provides insights into Criegee chemistry using a global chemical transport model.



ARTICLE

Global-scale analysis of the effect of gas-phase Criegee intermediates (CIs) to the sulphate aerosol formation: General trend and the importance of hydroxy radical decomposed from vibrationally-excited CIs

Received 00th January 20xx,
Accepted 00th January 20xx

DOI: 10.1039/x0xx00000x

Hiroo Hata^{*a}, Yuya Nakamura^b, Jairo Vazquez Santiago^a, and Kenichi Tonokura^c

Stabilised Criegee intermediates (sCIs), which are formed in the atmosphere through the ozonolysis of alkenes, are known precursors of sulphate aerosols ($\text{SO}_4^{2-}(\text{p})$). Several previous studies have focused on the kinetics of sCI-related chemistry using both experimental and theoretical methods. Nonetheless, detailed evaluations of how the sCI affects global-scale $\text{SO}_4^{2-}(\text{p})$ formation using chemical transport models (CTMs) have rarely been conducted. In this study, the impact of sCIs on $\text{SO}_4^{2-}(\text{p})$ and other particulate matter was estimated using a global CTM by implementing approximately 100 chemical reactions associated with CIs-chemistry. The results suggest that sCIs contribute maximally less than 0.5% in remote areas, such as Amazon rainforests, middle Africa, and Australia. This value is lower than the previously estimated value, despite certain kinetic parameters related to CI chemistry being provisional due to insufficient data. Future work should focus on obtaining these kinetic parameters through experimental studies or theoretical calculations. The sCI that contributed the most to $\text{SO}_4^{2-}(\text{p})$ formation was *E*-methyl glyoxal-1-oxide, which is generated by the ozonolysis of methyl vinyl ketone owing to its low-rate constant for the loss reaction of unimolecular decomposition and water vapour. The change in $\text{SO}_4^{2-}(\text{p})$ enhanced the formation of secondary organic aerosol, whereas the reactions of the sCIs and NO_2 degraded the formation of nitrate radicals. The results of the sensitivity analyses showed that in highly industrialised sites in China and India, OH radicals formed by the unimolecular decomposition of vibrationally excited CIs (vCIs) contributed to $\text{SO}_4^{2-}(\text{p})$ formation, which maximally accounted for nearly ten times more than that of sCIs, whereas the importance of vCIs and sCIs to $\text{SO}_4^{2-}(\text{p})$ formation were estimated to be almost equal in rural and remote sites. The estimated sCI loss by HNO_3 and organic acids was comparable to that of the unimolecular decomposition of sCIs and scavenging by water. This study provides full insight into the impact of gas-phase CIs chemistry on the global-scale atmosphere.

Introduction

Sulphate aerosol ($\text{SO}_4^{2-}(\text{p})$) is known as the nuclei of fine particulate matter ($\text{PM}_{2.5}$), which has negative impacts on human health¹⁻³ and contributes to the positive and negative radiative forcing.⁴⁻⁶ As described in Fig. 1, the ozonolysis of alkenes forms primary molozonide (POZ) and decomposes to

vibrationally-excited Criegee intermediates (vCIs) and carbonyl species.⁷⁻¹¹ The vCIs then decompose to form hydroxy radicals (OH) or release energy through quenching in ambient air to form stabilised Criegee intermediates (sCIs).⁷⁻¹³ The sCIs are known strong oxidisers in the atmosphere, reacting with several air pollutants such as sulphur dioxide (SO_2), nitrogen oxides (NO_x), and organic acids.⁷⁻¹¹ Especially since the rate constant of the reaction between sCIs and SO_2 , which finally transforms into $\text{SO}_4^{2-}(\text{p})$, was estimated to be high (approximately $10^{-11} \text{ cm}^3 \text{ molecule}^{-1} \text{ s}^{-1}$),⁷⁻¹¹ sCIs have been considered as one of the main contributors of atmospheric $\text{SO}_4^{2-}(\text{p})$ formation, and several studies analysed the impact of sCIs on $\text{SO}_4^{2-}(\text{p})$ formation on both a regional and global scale using chemical transport models (CTM). Sarwer et al. included sCI-related chemical reactions to the CTM and estimated the contribution of sCIs to $\text{SO}_4^{2-}(\text{p})$ formation, concluding that sCIs contributed 20% to 75% of total $\text{SO}_4^{2-}(\text{p})$ formation in the U.S.¹⁴ Percival et al. conducted regional and global analyses of the effect of sCIs on $\text{SO}_4^{2-}(\text{p})$ formation, and they concluded that the contribution of sCIs is as high as that of gas-phase oxidation of OH, especially in urban areas, although global CTM could not resolve the impact of sCIs on $\text{SO}_4^{2-}(\text{p})$ formation in the urban area due to the averaged

^a Research Institute of Science for Safety and Sustainability, National Institute of Advanced Industrial Science and Technology (AIST), 16-1 Onogawa, Tsukuba, Ibaraki 305-8569, Japan.

^b Department of Global Agricultural Sciences, Graduate School of Agricultural and Life Sciences, The University of Tokyo 1-1-1, Yayoi, Bunkyo-ku, Tokyo 113-8657, Japan.

^c Department of Environment Systems, Graduate School of Frontier Sciences, The University of Tokyo, Kashiwanoha 1-5-1, Kashiwa, Chiba 277-8563, Japan.

† ORCID:

Hiroo Hata: 0000-0002-3961-5593

Yuya Nakamura: 0009-0006-9459-6707

Jairo Vazquez Santiago: 0000-0002-2416-2317

Kenichi Tonokura: 0000-0003-1910-8508

Corresponding author:

Hiroo Hata: hata-hiroo@aist.go.jp; Tel: +81-80-2212-2713;

Electronic Supplementary Information (ESI) available: [Additional information cited in this paper is provided in the Supporting Information (SI_esatmos2023.pdf)]. See

DOI: 10.1039/x0xx00000x



emissions in each calculated grid.¹⁵ On the other hand, Nakamura et al. reported negligible contributions of sCl_s to SO₄²⁻(p) formation in the Greater Tokyo Area (GTA), the metropolitan area of Japan.¹⁶ The estimated amount of sCl_s in GTA was consistent with a previous study that estimated the amount of sCl_s in the urban area of U.K.¹⁷ Our previous study suggested that isoprene-derived sCl_s enhance SO₄²⁻(p) formation in the forestry area of the Asian region, which was comparable to the rate of aqueous-S(IV) chemistries¹⁸ although Newland et al. suggested less importance of isoprene-derived sCl_s to SO₂ oxidation at the global scale.¹⁹ Vereecken et al. estimated several rate constants related to sCl_s using quantum chemical calculations combined with transition state theory, and showed the importance of the unimolecular decompositions of sCl_s to the total evaluation of sCl-related pollution by the global CTM.²⁰ Other several studies also evaluated the impact of sCl_s on atmospheric pollutants, such as SO₂, organic acids, and peroxy radicals, by CTM, sometimes combined with reaction rate coefficients derived from experiments and calculations using transition state theory.²¹⁻²⁵ The impact of the Cl chemistry on the atmosphere has not been analysed in detail. Most previous studies have investigated the atmospheric implications of the newly estimated rate constants or the impact of the specific kinetics by applying the global-CTM, especially focusing on the impact of sCl_s on SO₄²⁻(p) formation. However, their impact on other aerosols has rarely been investigated. In addition, vCl_s may have a more significant impact on SO₄²⁻(p) formation than sCl_s. Khan et al. suggested that the OH formation through the unimolecular decomposition of vCl_s maximally contributes 13% of OH formation in the terrestrial rainforest and boreal forest regions.¹⁰ Also, Nakamura et al.¹⁶ implied that the formation of SO₄²⁻(p) due to incorporation of sCl_s mainly came from the increase in OH concentration caused by the unimolecular decomposition of vCl_s, not the direct oxidation of SO₂ by sCl_s. Further studies should be conducted to investigate the role of vCl_s in SO₄²⁻(p) formation through a comparative analysis of the contributions of sCl_s and OH derived from vCl_s.

This study aimed to reveal the impact of Cl chemistry on SO₄²⁻(p) and other aerosol formations on a global scale and to compare the impact of sCl_s and vCl_s on SO₄²⁻(p) formation. This study comprised three steps: First, we applied the detailed sCl-related chemical mechanisms proposed by Nakamura et al.¹⁶ most of which were originally based on the reactions of Vereecken et al.²⁰ to the global-CTM to evaluate the effect of sCl_s on SO₄²⁻(p) formation on a global scale. Second, we investigated sCl_s impact on ionic and SOA formation in addition to SO₄²⁻(p) to show the cross-effect of sCl_s to other particulate species. Third, we conducted a sensitivity analysis to compare the contribution of SO₄²⁻(p) formation between sCl_s and OH derived from the unimolecular decomposition of vCl_s and the contribution of other sCl loss reactions. Although there have been many previous studies related to the impact of gas-phase reactions of sCl_s on the atmosphere using CTM, this study contributes to providing new insights into the atmospheric contribution of sCl_s and vCl_s, and the fundamental information of whole Cl chemistry.

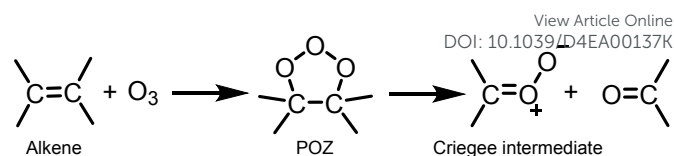


Figure 1: Reactions of alkene ozonolysis and formation of CI.

Methodology

Global chemical transport modelling

The Goddard Earth Observing System Chemistry model (GEOS-Chem v14.2.3)²⁶ was used as the global CTM. The modern-era retrospective analysis for research and applications version 2 (MERRA2) was used as the meteorological input with a grid resolution of 2° × 2.5° (latitude × longitude) holding 72 vertical layers from troposphere to stratosphere.²⁷ Emission inventories provided by the harmonized emissions component (HEMCO) system were applied in this study.²⁸ Briefly, the emissions database for the community emissions data system (CEDsv2) was chosen for anthropogenic emissions,²⁹ hemispheric transport of air pollution (HTAPv3) was chosen for ship emissions,³⁰ monthly mean data of the Aviation Emissions Inventory (AEIC2019) was chosen for aircraft emissions,³¹ global fire emissions database (GFED) was chosen for biomass burning,³² Aerosol Comparisons between Observations and Models (AeroCom) was selected for the SO₂ emissions from volcanoes,³³ and the off-line model of emissions of gases and aerosols from nature (MEGAN) was chosen for BVOC emissions.³⁴ The targeted period calculated in this study was spanned from 1st July 2018 to 31st December 2019. The first six months (1 July 2018 to 31st December 2018) were treated as the spin-up period, and the entire year of 2019 was treated as the analysis term. The reactions of the Criegee intermediates (CIs) were added to the full chemistry module of the kinetic pre-processor (KPP). The added CI reactions were based on Nakamura et al., who analysed the impact of sCl_s on SO₄²⁻(p) formation in the GTA of Japan.¹⁶ Nakamura et al. cited several reaction kinetics from the findings of Vereecken et al., who determined the rate constants of sCl_s atmospheric reactions using quantum chemical calculations coupled with transition state theory.²⁰ The default KPP has already implemented the chemical reactions of CIs generated by ethylene and propene. In this study, those CI-chemistries were excluded to unify the reactions applied in Nakamura et al.¹⁶ The details of the added reactions are described in a later section.

Validation of the modelling results using satellite data

Validation of modelling results at regional scales is typically conducted through comparisons with ground observations. However, considering the coarse resolution of our analysis (2° × 2.5°), a direct comparison with ground observations is challenging. The results were validated by comparison with satellite observations from the tropospheric monitoring instrument (TROPOMI)³⁵⁻³⁷. Alkenes, O₃, and SO₂ were the main species forming sCl_s and SO₄²⁻(p), and comparing these species would be ideal for model validation. Owing to the lack of satellite observations of alkenes, HCHO, which has been widely



used as an indicator of VOC emissions (including alkenes),³⁸ was used, along with tropospheric O₃ and SO₂. Level 2 data for HCHO, tropospheric O₃, and SO₂ were retrieved from COPERNICUS (O₃; spatial resolution: 30 × 30 km²)³⁹ and NASA Earth Observation Data (HCHO and SO₂; special resolution: 7 × 3.5 km²).⁴⁰ Datasets were screened based on the recommended quality flags (<0.5) to produce Level 3 data, solar zenith angle < 85°, and cloud fraction < 30%.³⁹ The TROPOMI data were re-gridded to equal the spatial resolution to that of GEOS-Chem (2° × 2.5°) via linear interpolation of the targeted grids. TROPOMI provides daytime data on the column densities of pollutants, which were compared with the daily average values calculated by GEOS-Chem. The determination factor (R²), root mean square error (RMSE), normalised mean bias (NMB), and normalised mean error (NME) were chosen as statistical indicators to verify the correlation between the observed and calculated results. Globally, five sites were selected for comparison: China (CHI), India (IND), South Africa (ZAF), Australia (AUS), and Bolivia (BOL: corresponding to the Amazon rainforests), where the impacts of sCIs were estimated to be high according to this study, the details of which are described in a later section. Detailed information on the five sites is provided in Table S1 of the Electronic Supplementary Information (ESI).

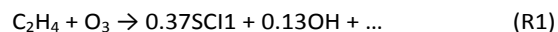
Incorporated chemical reactions

The chemical mechanisms of the ozonolysis reactions of 8 alkenes (ethylene (C₂H₄), propene (PRPE), methyl vinyl ketone (MVK), methacrolein (MACR), isoprene (ISOP), pinene (MTPA), other monoterpenes (MTPO), and limonene (LIMO)), unimolecular reactions sCIs, and eight types of bimolecular reactions between sCIs and air pollutants (water monomer (H₂O), water dimer ((H₂O)₂), nitrogen dioxide (NO₂), sulphur dioxide (SO₂), nitric acid (HNO₃), formic acid (HCOOH), acetic acid (CH₃COOH), and the organic acids holding more than C₃-chain (RCOOH)) were incorporated to KPP. There were eight types of sCIs generated from alkene ozonolysis: formaldehyde oxide (SCI1), acetaldehyde oxide (SCI2), methyl vinyl ketone oxide (SCI3), methacrolein oxide (SCI4), two types of pinene oxides (SCI5 and SCI6), methyl glyoxal-1-oxide (SCI7), and methyl glyoxal-2-oxide (SCI8), of which all the sCIs aside from SCI1 hold *E*- and *Z*-isomers. Detailed structures of the sCIs are shown in Fig. S1 of the ESI. Most of the chemical mechanisms and rate constants are cited from Nakamura et al.¹⁶ Additionally, they analysed the effect of sCIs on SO₄²⁻(p) formation in the GTA using the community multiscale air quality modelling system (CMAQ)⁴¹ with the SAPRC-07 chemical mechanism,⁴² and several expressions of the chemical species were different from those of KPP. The corresponding species were chosen to substitute the SAPRC-07 components with KPP. The summaries of the added reactions are summarised in Tables S2 to S10 of the ESI.

Alkene ozonolysis

Table S11 of the ESI lists the incorporated alkene ozonolysis reactions and rate constants of which those information were originally cited from Master Chemical Mechanism (MCM).⁴³ The default reactions of alkenes and O₃ defined in KPP were substituted by the reactions listed in Table S11 because MCM

holds more detailed chemistries of sCIs generation. The 15 sCI structures shown in Fig. S1 of the ESI, including *E*- and *Z*-isomers of several sCIs, were generated from the ozonolysis of the alkenes. The branching ratio of *E*- and *Z*-isomers was assumed to be 0.5.^{16,18} The reactions of alkene ozonolysis reactions are shown in Fig. S1, which depicts the generation of the sCIs and OH. For example, ethylene ozonolysis is defined as follows:



The formation of OH from R1 can be considered the end product of the unimolecular decomposition of vCIs.

Unimolecular decomposition of sCIs

Unimolecular decomposition of sCIs is one of the major pathways of sCI loss,²⁰ and Table S2 lists the chemical mechanisms of the unimolecular reaction of sCIs and their kinetic parameters. Three types of unimolecular decompositions, 1,3-ring closure, 1,4-H-migration, and 1,5-ring closure, were considered, and the details of these reactions are described by Vereecken et al.²⁰

Reactions of sCIs with H₂O and (H₂O)₂

The reactions of sCIs with water monomers (H₂O) and dimers ((H₂O)₂) are also one of the major paths for the loss of sCIs; Tables S3 and S4 of the ESI list the chemical mechanisms and kinetic parameters of the reaction. Note that the kinetic parameters of the reactions of sCIs and (H₂O)₂ depend on the ratio of H₂O to (H₂O)₂ in the atmosphere, which is described by the equilibrium constant *K_w*, expressed by Eq. 1 according to a previous study.⁴⁴

$$K_w = \frac{[(\text{H}_2\text{O})_2]}{[\text{H}_2\text{O}]^2} \quad (1)$$

Further details of the derivation of the rate constants listed in Table S4 have been described in a previous study.¹⁶

Reactions of sCIs with SO₂, NO₂, HNO₃, and organic acids

Tables S5–S11 show the incorporated reactions and kinetic parameters of the reactions between sCIs and SO₂, NO₂, HNO₃, and organic acids. The main difference from Nakamura et al. is the definition of the reactions between sCIs and NO₂. In a previous study,¹⁶ the products of the sCIs + NO₂ were defined as NO₃ and aldehydes (or ketones). Caravan et al.⁴⁵ found out that the main product of the reaction is sCIs-NO₂ adduct, and only approximately 30% of sCIs-NO₂ adduct decomposes to NO₃ and aldehyde (or ketone), indicating that NO₃ formation through sCIs + NO₂ reaction was overestimated in Nakamura et al.¹⁶ For this reason, in this study, we applied to multiply 0.3 to NO₃ and aldehyde (or ketone) as the stoichiometric factor to incorporate the finding of Caravan et al.⁴⁵

Sensitivity analysis to compare the contribution on SO₄²⁻(p) formation between sCIs and vCIs

Sensitivity analysis was conducted to reveal the important CI-related reaction scheme for SO₄²⁻(p) formation. Seven scenarios were used to evaluate sensitivity: unimolecular decomposition of vCIs (S1), reactions of sCIs with SO₂ (S2), unimolecular decomposition of sCIs (S3), reactions of sCIs with water (S4), reactions of sCIs with NO₂ (S5), reactions of sCIs with HNO₃ (S6), and reactions of sCIs with organic acids (S7). The reactions



evaluated in scenarios S1 and S2 contributed to $\text{SO}_4^{2-}(\text{p})$ formation through SO_2 oxidation by OH or sCl_s. The other scenarios (S3–7) were loss reactions of sCl_s, which indirectly contributed to $\text{SO}_4^{2-}(\text{p})$ formation. Note that although scenario S1 focuses on the contribution of vCl_s to $\text{SO}_4^{2-}(\text{p})$ formation, the exact species of vCl_s are not defined in the chemical mechanism of this study. This is because vCl_s are intermediate species in the ozonolysis reaction of alkenes and are either immediately decomposed into OH or stabilised through collisions with bath gas to form sCl_s. Thus, scenario S1 only calculates the total sensitivity to ozonolysis minus the sensitivity to the reactions of sCl_s. To evaluate the contribution of each process to $\text{SO}_4^{2-}(\text{p})$ formation, the sensitivity, S_i , of reaction scheme i was formulated as follows:

$$S_i = \frac{k_i}{[\text{SO}_4^{2-}(\text{p})]} \frac{\delta[\text{SO}_4^{2-}(\text{p})]}{\delta k_i} \quad (2),$$

where k_i is the rate constants of the targeted reaction scheme i , and δk_i is the functional derivative of k_i . $[\text{SO}_4^{2-}(\text{p})]$ refers to the column density of $\text{SO}_4^{2-}(\text{p})$ in the scenario with Criegee-chemistry, and $\delta[\text{SO}_4^{2-}(\text{p})]$ refers to the change of $[\text{SO}_4^{2-}(\text{p})]$ after the reaction rates were multiplied by $(1 + \delta k_i/k_i)$. In this study, the value of $\delta k_i/k_i$ was set to 0.1. For example, the sensitivity of sCl_s and SO_2 reactions to $\text{SO}_4^{2-}(\text{p})$ formation was calculated by multiplying the rate constants of all sCl_s + SO_2 reactions by 1.1 and investigating the change in the column density of $\text{SO}_4^{2-}(\text{p})$. In terms of sensitivity scenario S1, the rate constants of the ozonolysis reactions of alkenes were multiplied by 1.1; however, this operation also led to the enhancement of later sCl_s-related reactions, which resulted in including both the effects of vCl_s and sCl_s on the sensitivities of $\text{SO}_4^{2-}(\text{p})$ and other aerosol formations. To account for this problem, another scenario, S8, was calculated, which contains the operation of multiplying 1.1 by the rate constants of all sCl_s-related chemical reactions. The results of scenario S1 were then subtracted by the results of scenario S8 to ensure that S1 held only the sensitivities of the vCl_s to aerosol formation. In the results and discussion section, the sensitivity of S1 contains the subtracted result for scenario S8.

Results and discussion

Evaluation of the modelling performance comparing with the observed data of TROPOMI

Fig. 2 shows the relationships between the observed and modelled column densities of O_3 , HCHO, and SO_2 . According to Fig. 2(a) and (b), O_3 and HCHO showed high determination coefficients with $R^2 = 0.83$ and 0.57, respectively, while the value of R^2 for SO_2 was 0.37, indicating a moderate linear correlation between the observed and modelled results. The slopes of all three chemicals were less than 1.0 with SO_2 showing the lowest value, followed by O_3 and HCHO. This suggests that the modelled results underestimated observation especially in SO_2 . One of the emission sources of SO_2 is anthropogenic activities, and thus, the emission of SO_2 is highly

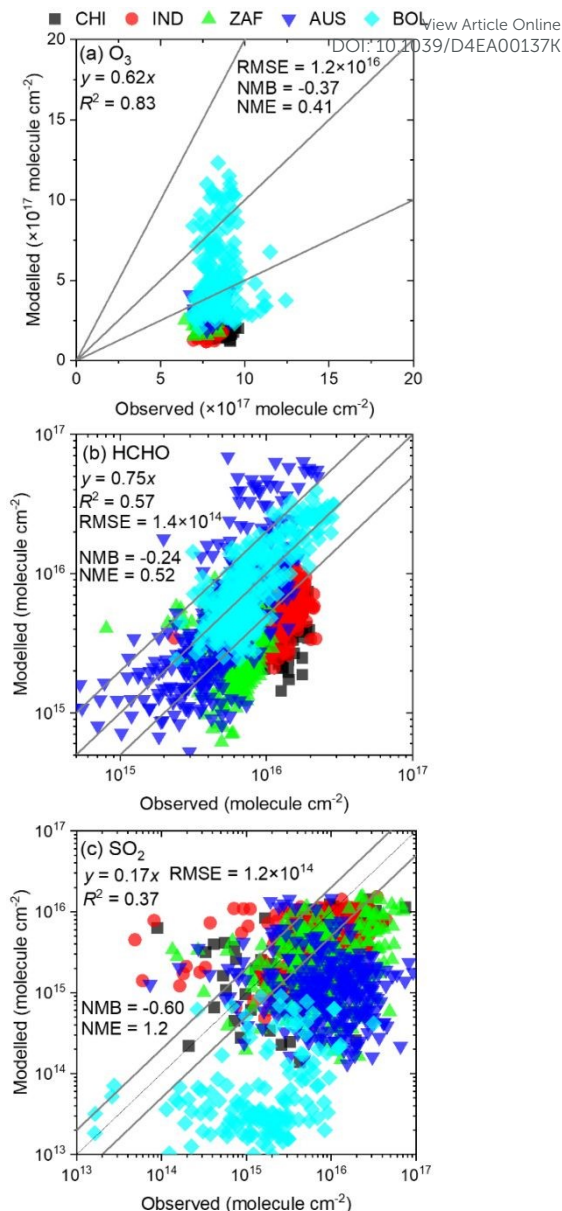


Figure 2: Comparison of observed and modelled results of the column density of (a) tropospheric O_3 , (b) HCHO, and (c) SO_2 . HCHO and SO_2 are shown in the scale of common logarithm for readability.

dependent on time. Fig. 2 shows a comparison between the 1-h observed data by TROPOMI during the daytime and the daily averaged modelled results by GEOS-Chem, and this is the reason why the modelled results underestimated the daytime observational results. Similarly, O_3 exhibited higher concentrations during daytime compared to the nighttime, as it is generated by the photochemical reaction of NO_2 and the related HO_x cycle; thus, the modelled results underestimated the observed data due to the large concentration difference between daytime and nighttime. In contrast, the sources of HCHO are mostly secondary products of the atmospheric oxidation of VOCs including nocturnal reactions. Therefore, HCHO is produced at all times of the day, leading to a relatively small underestimation of the modelled HCHO compared to the observed results. In addition, the results obtained using



TROPOMI were linearly interpolated to fit the grid resolution of GEOS-Chem, which may have caused errors between the observed and calculated results. The comparisons between TROPOMI and GEOS-Chem were conducted using column density rather than the surface mixing ratio, which may have contributed to error accumulation across vertical layers. These complex analyses resulted in relatively large discrepancies between TROPOMI and GEOS-Chem. Additionally, the accuracy of emission inventories for air pollutants is not perfect, as these inventories are estimated using statistical methods. Collectively, these factors influenced the observed differences between TROPOMI and GEOS-Chem. Overall, although discrepancies were observed between TROPOMI and GEOS-Chem for SO₂, the calculated column densities of O₃, HCHO, and SO₂ correlate with the observed data in terms of determination coefficients, indicating acceptable agreement between the datasets.

Distribution of sCIs formed by alkene ozonolysis in 2019

Fig. 3 shows the annual average column density of the total sCIs in 2019 calculated using GEOS-Chem. The column density was high in the equatorial regions of the Amazon rainforests, Australia, Middle Africa, Southeast Asia, and some Middle to North American countries, including the U.S. and Mexico. The column densities of the precursors of the sCIs, O₃, and total alkenes are shown in Fig. S2 of the ESI. In a comparison between Fig. 3 and Fig. S2, the abundance of sCIs was nearly correlated with the abundance of alkenes. Figs. S3–S8 of the ESI show the column density of the detailed species of the sCIs, and Fig. S9 provides a detailed description of the alkene species. According to Figs. S3–S8, SCI1 (formaldehyde oxide), ESCI3 (*E*-methyl vinyl ketone oxide), ESCI4 (*E*-methacrolein oxide), and ESCI7 (methyl glyoxal-1-oxide) were the main contributors of the total amount of sCIs. While SCI1 is generated from both anthropogenic and biogenic alkenes, ESCI3 and ESCI4 are generated from isoprene, a biogenic alkene, and ESCI7 is generated from methyl vinyl ketone, a byproduct of isoprene oxidation. The column density of ESCI7 was the highest among all sCIs. The high concentration of ESCI7 resulted from the low rates of unimolecular decay and ESCI7 and water reactions. Because of the geometrical structure of ESCI7, only 1,3-ring-closure was considered for the unimolecular isomerisation of ESCI7. For example, ESCI3, which is generated by isoprene ozonolysis, involves two unimolecular isomerisation processes: 1,3-ring closure and 1,4-H-migration. The rate constants of the 1,3-ring closure for ESCI7 and ESCI3, and of 1,4-H-migration for ESCI3 at 298 K were 0.058 s⁻¹, 0.0040 s⁻¹, and 51 s⁻¹, respectively, calculated using the values listed in Table S2 of the ESI. Similarly, assuming the concentration of water at 298 K as 8.3 × 10¹⁷ molecule cm⁻³,⁴⁶ the reaction rates of SCI1, ESCI3, ESCI4, and ESCI7 with water are calculated to be 2866 s⁻¹ (716 s⁻¹ for H₂O and 2150 s⁻¹ for (H₂O)₂), 0.525 s⁻¹ (0.065 s⁻¹ for H₂O and 0.460 s⁻¹ for (H₂O)₂), 668 s⁻¹ (158 s⁻¹ for H₂O and 510 s⁻¹ for (H₂O)₂), and 22.0 s⁻¹ (2.50 s⁻¹ for H₂O and 19.5 s⁻¹ for (H₂O)₂), respectively calculated by the values listed in Tables S3 and S4 of the ESI. Thus, because of the relatively high concentration of MVK in the atmosphere, which is shown in Fig. S9 of the ESI, and because of lower reaction rate in the main loss processes, which enables a longer atmospheric lifetime, ESCI7 showed a high concentration in the atmosphere, as discussed by Vereecken et al.²⁰ For similar reasons, *E*-isomers of sCIs are more dominant than *Z*-isomer because

of the high reactivity of *Z*-isomers to unimolecular isomerization.²⁰ Some of the previous studies suggested the importance of (*E*- and *Z*-)SCI3 and (*E*- and *Z*-)SCI4 as atmospheric oxidisers because SCI3 and SCI4 are directly generated from the ozonolysis of isoprene, which is the most relevant VOCs on a global-scale.^{18,19} Nevertheless, this study showed the potential importance of ESCI7 as the most relevant atmospheric oxidiser among the sCIs owing to its long atmospheric lifetime. Therefore, further studies on the kinetics of ESCI7 in the atmosphere should be conducted in the future. Fig. S9 suggests that ethylene, isoprene, and methyl vinyl ketone are the relevant alkenes in the atmosphere, and that ethylene is emitted from both anthropogenic and biogenic sources. Combining these results, most sCIs are formed from biogenic sources, particularly isoprene, on a global scale. The seasonal trend of the column density of sCIs in 2019 is shown in Fig. S10 of the ESI, where the year is divided into four seasons: January–March (JFM), April–June (AMJ), July–September (JAS), and October–December (OND). In the Northern Hemisphere, the seasons of AMJ and JAS exhibit relatively high concentrations, particularly in the south-eastern regions of the United States and the eastern part of Russia (Siberia). This is because AMJ and JAS correspond to warm to hot seasons in the Northern Hemisphere, during which high amounts of BVOCs are emitted. Conversely, except for the Amazon rainforest, the seasons of JFM and OND show relatively high concentrations of sCIs in the Southern Hemisphere, also due to high-temperature seasons in those regions. Although the Amazon rainforest is located in the equatorial and Southern Hemisphere, its rainy seasons during JFM, AMJ, and OND result in JAS having the highest concentration of sCIs.

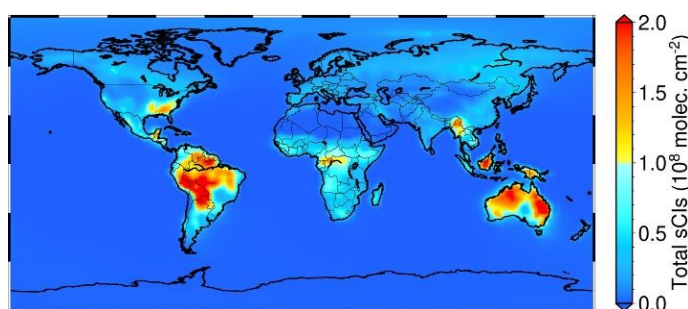


Figure 3: Annual-mean total column density of sCIs in 2019.

Impact of Criegee-chemistry on the sulphate formation

Fig. 4 shows the calculated results of the column densities of SO₄²⁻(p) for (a) annual-mean SO₄²⁻(p) (μg cm⁻²), (b) the change of SO₄²⁻(p) due to Criegee-chemistry (μg cm⁻²), and (c) the ratio of the change of SO₄²⁻(p) (%), respectively. According to Fig. 4(a), SO₄²⁻(p) is distributed globally, but its concentration is high in the northern hemisphere, where the countries such as China, India, and Middle Eastern countries are located, which results in high SO₂ emissions from the burning of fossil fuels, as shown in Fig. S2(b). According to Fig. 4(b), the change in SO₄²⁻(p) was significant in China and India, both of which emit substantial amount of SO₂ due to the of fossil fuel combustion, and in the Amazon rainforests, middle to south Africa, and Australia, which are dominated by forests, causing high BVOC emissions and high sCIs concentrations, as shown in Fig. 3. Thus, the effect of Criegee-chemistry on SO₄²⁻(p) formation was high in high-SO₂ and BVOC emissions. Fig. 4(c) demonstrates that the



contribution of Criegee-chemistries to the rate of change of $\text{SO}_4^{2-}(\text{p})$ is maximally less than 0.5% in the Amazon rainforests, Australia, and middle Africa, of which the value is not drastic in terms of the air pollution issue. The percentage contribution of Criegee-chemistry to $\text{SO}_4^{2-}(\text{p})$ formation is high in those regions because the background concentration of $\text{SO}_4^{2-}(\text{p})$ is low in remote areas, so the incorporation of the Criegee-chemistry showed higher responsiveness in those regions. As mentioned above, SCI1, ESCI3, ESCI4, and ESCI7 were the dominant sCIs on the global scale, and these four sCIs mainly contributed to the formation of $\text{SO}_4^{2-}(\text{p})$. Seasonal trends in the column density of $\text{SO}_4^{2-}(\text{p})$ are shown in Figs. S11–S14 of the ESI, with the seasons divided in the same manner as in Fig. S10: January–March (JFM), April–June (AMJ), July–September (JAS), and October–December (OND). The absolute changes in $\text{SO}_4^{2-}(\text{p})$ in the eastern part of China during JFM and OND, which correspond to the cool to cold seasons, show a significant increase due to high SO_2 emissions driven by increased fossil fuel demand. In the Amazon rainforest, the changes in $\text{SO}_4^{2-}(\text{p})$ are highest during JAS, as JFM, AMJ, and OND coincide with the rainy seasons. The concentration of sCIs is also highest during JAS, as discussed in the previous section.

The contributions of sCIs to the change in $\text{SO}_4^{2-}(\text{p})$ shown in Fig. 4(c) are lower than the results of Newland et al., who evaluated the impact of monoterpene-derived sCIs on $\text{SO}_4^{2-}(\text{p})$ formation, which suggested that sCIs from monoterpenes account for 1.2% of annual $\text{SO}_4^{2-}(\text{p})$ formation in the terrestrial tropics.²⁴ The difference might come from the included sCIs chemical reactions. Newland et al. considered the reactions of sCIs with SO_2 , H_2O (monomers), and the unimolecular decomposition of sCIs, whereas this study included additional reactions involving $(\text{H}_2\text{O})_2$, NO_2 , HNO_3 , and three organic acids. The inclusion of these additional reactions would lower the concentration of sCIs, thereby leading to slower oxidation of SO_2 . Caravan et al. also suggested a 1–10% contribution of $\text{SO}_4^{2-}(\text{p})$ formation in the terrestrial tropics from isoprene-derived Criegee intermediates (SCI3 in this study)²³, but for the same reason as Newland et al.²⁴, the estimated contribution might be overestimated.

Effect of Criegee-chemistry on $\text{NO}_3^-(\text{p})$, $\text{NH}_4^+(\text{p})$, and SOA formation

According to a previous study, the incorporation of Criegee-chemistry led to not only an increase in $\text{SO}_4^{2-}(\text{p})$ but also a change in other particulate species owing to the change in ionic balance and the enhancement of particle formation through nucleation around the surface of $\text{SO}_4^{2-}(\text{p})$.¹⁸ These particulate species include nitrate aerosol ($\text{NO}_3^-(\text{p})$), ammonium aerosol ($\text{NH}_4^+(\text{p})$), and secondary organic aerosol (SOA), which is defined in ISORROPA II implemented in GEOS-Chem⁴⁷. Fig. 5 shows the change in the composition of particulate matter at five sites: CHI, IND, ZAF, AUS, and BOL (Table S1), which showed high $\text{SO}_4^{2-}(\text{p})$ formation caused by Criegee-chemistry incorporation, as shown in Fig. 4. According to Fig. 5(a), all sites showed an increase in $\text{SO}_4^{2-}(\text{p})$ and SOA, of which the results are consistent with the previous study of Hata et al.¹⁸ Budisulistiorini et al. suggested that SOA formation strongly

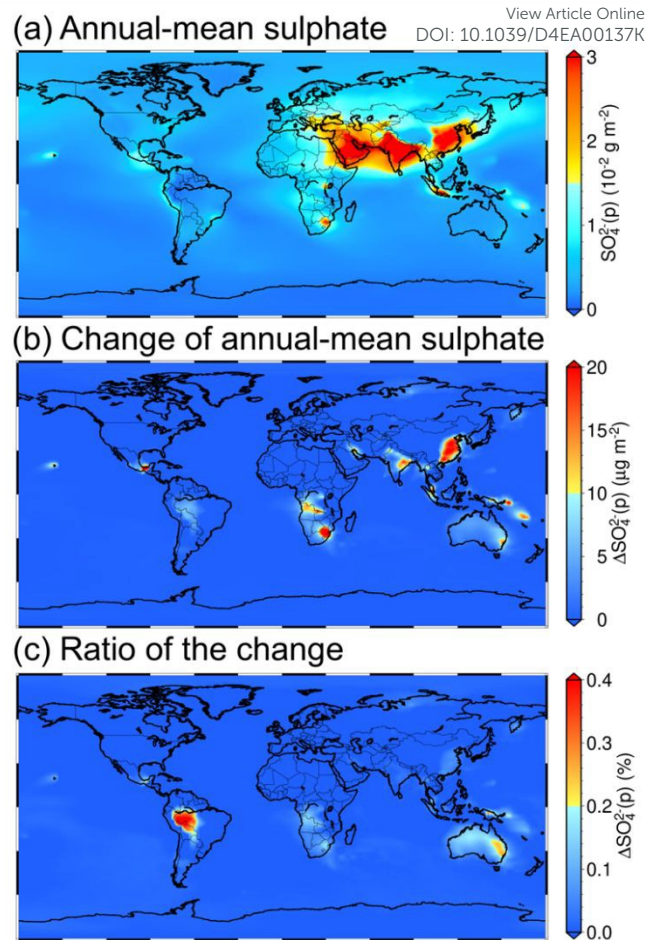


Figure 4: Annual-mean column density of (a) sulphate (g m^{-2}), (b) the change of the column density of sulphate before and after the introduction of Criegee-chemistry (mg m^{-2}), and (c) the rate of change of sulphate before and after the introduction of Criegee-chemistry (%).

correlates with the ambient concentration of $\text{SO}_4^{2-}(\text{p})$, and 25% decrease in $\text{SO}_4^{2-}(\text{p})$ induces a 70% decrease in SOA.⁴⁸ For this reason, the high increase in SOA shown in Fig. 5(a) is due to the increase in $\text{SO}_4^{2-}(\text{p})$ induced by Criegee-chemistry incorporation. On the other hand, a decrease in $\text{NO}_3^-(\text{p})$ was estimated for all the analysed sites, which is inconsistent with the results of a previous study by Hata et al.¹⁸ Hata et al. treated sCIs + NO_2 reactions to completely form NO_3 radicals. However, according to the findings of Caravan et al., only 30% of NO_3 was estimated to be formed by sCIs + NO_2 reactions, and remained NO_2 was considered to form the additives of sCIs- NO_2 .⁴⁵ This new finding was implemented in this study. Thus, the formation of sCIs- NO_2 additives resulted in NO_2 removal from the atmosphere, leading to a decrease in $\text{NO}_3^-(\text{p})$. As shown in Fig. 5(a), the decrease in $\text{NO}_3^-(\text{p})$ was large in CHI and IND, where highly anthropogenic air pollutants were likely to be emitted, as implied by the column density of SO_2 (Fig. S2(b)). These two sites emitted high amounts of NO , subsequently forming NO_2 via a reaction with O_3 , which caused a strong decline in $\text{NO}_3^-(\text{p})$ due to NO_2 removal by sCIs. This suggests that in areas with high emission, the increases in $\text{SO}_4^{2-}(\text{p})$ and SOA were cancelled by the reduction of $\text{NO}_3^-(\text{p})$, all of which were caused by Criegee-chemistry incorporation. In contrast, the decrease in $\text{NO}_3^-(\text{p})$ was low at



the remaining sites with relatively lower anthropogenic emissions. The behaviour of $\text{NH}_4^+(\text{p})$ differed at each site. Because NH_4^+ is the counter ion of SO_4^{2-} , NO_3^- , and other anion species, $\text{NH}_4^+(\text{p})$ increased when the total cations increased (ZAF and AUS) and decreased when the total cations decreased (CHI and IND). According to Fig. 5(b), the change in column densities of $\text{SO}_4^{2-}(\text{p})$, $\text{NO}_3^-(\text{p})$, $\text{NH}_4^+(\text{p})$, and SOA at the five sites ranged from -1.3% to 0.4% depending on the sites and species. The ratios were higher for AUS and BOL than for CHI and IND. This trend may have been due to the lower background concentrations of particulate species in the AUS and BOL. The lower anthropogenic emissions led to lower particulate species in the AUS and BOL, which have resulted in the high responsiveness to concentration fluctuations derived from Criegee-chemistry incorporation. In contrast, ZAF showed moderate anthropogenic emissions according to the column density of SO_2 (Fig. S2(b)), indicating an intermediate trend in the ratio (%) between the high- and low-emission sites.

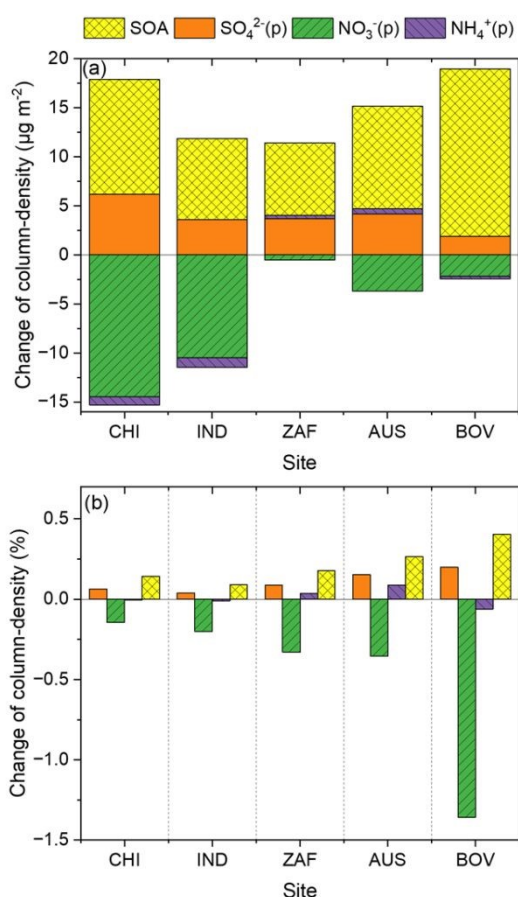


Figure 5: Cross-effects of the change of $\text{SO}_4^{2-}(\text{p})$ to $\text{NO}_3^-(\text{p})$, $\text{NH}_4^+(\text{p})$, and SOA by the introduction of Criegee-chemistry.

Sensitivity analysis of the rate constants of Criegee-inducing chemical reactions to the formation of sulphate aerosol

vCIs vs. sCIs: which CIs are important to $\text{SO}_4^{2-}(\text{p})$ formation?

Fig. 6 shows the results of the sensitivity analysis of the vCIs and sCIs (scenarios S1 and S2) for $\text{SO}_4^{2-}(\text{p})$ formation at the five sites estimated by Eq. 2. Fig. 6 suggests that vCIs contributed more to the formation of $\text{SO}_4^{2-}(\text{p})$ than sCIs at all analysed sites. In areas with high emissions CHI, IND, and ZAF, the contribution of vCIs was much higher than that of sCIs, whereas in sites with lower anthropogenic emissions, AUS and BOL, the contribution was equal. At sites with high to moderate anthropogenic emissions, such as CHI, IND, and ZAF, bimolecular reactions between sCIs and other pollutants, such as NO_2 and HNO_3 , frequently occur, which degrade the oxidation of SO_2 by sCIs. Thus, a relatively high vCIs contribution to $\text{SO}_4^{2-}(\text{p})$ formation was estimated in these sites. In contrast, in AUS and BOL, low concentrations of air pollutants led to a relatively high contribution of sCIs to $\text{SO}_4^{2-}(\text{p})$ formation in AUS and BOL, which was almost comparable to the contribution from vCIs. Previous studies have separately investigated the atmospheric roles of vCIs and sCIs. Khan et al. suggested an approximate 13% contribution of OH formation from the unimolecular reactions of vCIs in the terrestrial rainforests and boreal forest regions¹⁰. Numerous studies have focused on the importance of sCIs in the formation of $\text{SO}_4^{2-}(\text{p})$ in both remote and urban areas^{14-18, 20}. However, the contribution of $\text{SO}_4^{2-}(\text{p})$ formation in vCIs and sCIs has not been compared in previous studies. This study quantitatively evaluates their contributions through a detailed sensitivity analysis. The OH from the unimolecular decomposition of vCIs is a more dominant oxidiser of SO_2 than the direct oxidation of SO_2 by sCIs, especially in urban areas.

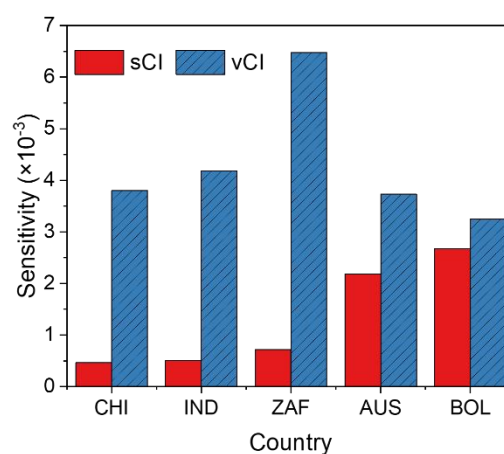


Figure 6: Sensitivities of sCI- and vCI-chemical reactions to $\text{SO}_4^{2-}(\text{p})$ formation in the five analysed sites.

Sensitivities of the sCI-loss reactions via unimolecular decomposition and water

Fig. 7 shows the sensitivity of the unimolecular decomposition of the sCIs and the reaction of the sCIs with water to the formation of $\text{SO}_4^{2-}(\text{p})$ (scenarios S3 and S4). Most of the results showed a negative impact on $\text{SO}_4^{2-}(\text{p})$ formation because both the unimolecular decomposition of sCIs and the reaction of sCIs with water are sCI-scavenging reactions, leading to a decrease in the total amount of $\text{SO}_4^{2-}(\text{p})$ formation. Only the sensitivity of the unimolecular decomposition of sCIs in CHI showed a



positive value, possibly because the products of the unimolecular decomposition of sCIs included OH and the precursors of OH, such as aldehydes, which surpassed the negative effect of the consumption of sCIs. At all the analysed sites, the sensitivity of the reaction of sCIs and water was higher than that of the unimolecular decomposition of sCIs, indicating that the reaction of sCIs with water is more important for the consumption of sCIs and subsequent reduction of $\text{SO}_4^{2-}(\text{p})$ formation. Only BOL showed high sensitivity to the unimolecular decomposition of sCIs, which was almost equal to the sensitivity of water. This was due to the abundant sCIs derived from BVOCs in the BOL, which are in the terrestrial Amazon rainforests and have intense BVOCs emissions (Fig. S9). Vereecken et al. showed that sCIs from BVOCs tend to be lost faster by unimolecular decomposition than sCIs from AVOCs²⁰, leading to high sensitivity of the unimolecular reactions of sCIs. Cox et al.¹⁷ and Vereecken et al.²⁰ estimated the contributions of sCI-loss reactions in urban and suburban areas and found that the contributions of unimolecular decomposition and water scavenging of sCIs are equal or that unimolecular decomposition is higher, and the results are opposite to the results shown in Fig. 7. This study investigated the temperature dependence of the ratio of $\text{H}_2\text{O}/(\text{H}_2\text{O})_2$, which differs from the results of previous studies. Furthermore, the contributions of the two sCI-loss processes were evaluated using the functional derivative of the sensitivity equation defined in Eq. 2, while previous studies estimated the contributions by comparing the ratio of the rate constants between unimolecular decomposition and water weighed by the ambient concentrations.^{17,20} Therefore it is difficult to completely compare the results between this study and previous studies due to the difference in the definition of the sensitivity and the sCI-chemical reactions included in this study.

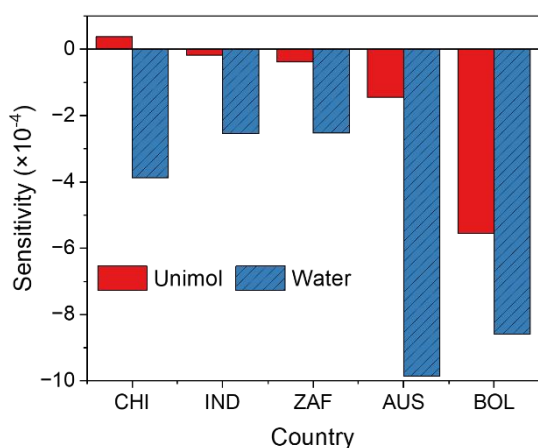


Figure 7: Sensitivities of sCI-loss reactions by the unimolecular decomposition of sCIs (Unimol) and by the reaction of sCIs and water in the five analysed sites.

Sensitivities of the sCI-loss reactions via NO_2 , HNO_3 , and organic acids

Fig. 8 shows the sensitivities of the sCI-loss reactions by NO_2 , HNO_3 , and organic acids to $\text{SO}_4^{2-}(\text{p})$ formation (scenarios S5, S6, and S7). At all analysed sites, the sensitivity of NO_2 showed a

positive contribution to $\text{SO}_4^{2-}(\text{p})$ formation, whereas the sensitivities of HNO_3 and organic acids showed negative contributions. We applied the reaction of sCIs and NO_2 to form 30% of NO_3 , according to Caravan et al.⁴⁵ NO_3 is known as a nocturnal oxidiser and enhances the HO_x cycle,⁴⁹ and this scheme might contribute to the positive sensitivity of NO_3 to $\text{SO}_4^{2-}(\text{p})$ formation. However, the sensitivities of the sCI-loss reactions of HNO_3 and organic acids were negative because these species consume sCIs, which degrade the sCIs + SO_2 reactions. It is important to note that the negative sensitivities of the reactions of HNO_3 and organic acids with sCIs to $\text{SO}_4^{2-}(\text{p})$ formation were of the same order of magnitude as those of unimolecular decomposition and water reactions, especially at remote sites, including AUS and BOL. Therefore, the presence of HNO_3 and organic acids in the atmosphere led to the degradation of $\text{SO}_4^{2-}(\text{p})$ formation through oxidation by sCIs, which are as significant as the unimolecular decomposition of sCIs and the reaction of sCIs and water.

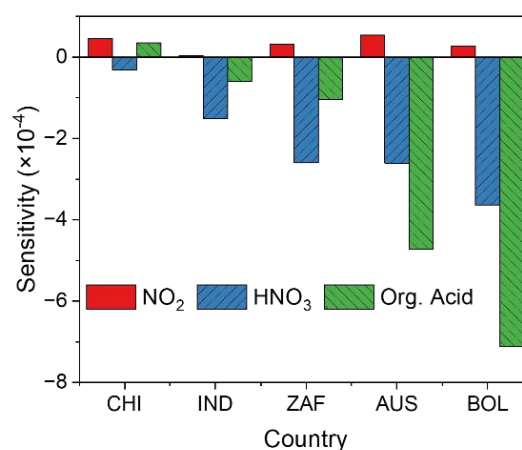


Figure 8: Sensitivities of the reactions of sCIs with NO_2 , HNO_3 , and organic acids (described as Org. Acid in the figure).

Overall conclusions of the sensitivity analyses

This study shows the sensitivity of the sCI chemical reactions to the formation of $\text{SO}_4^{2-}(\text{p})$ according to the detailed sensitivity analysis method defined by Eq. 2. The results suggest that in all the analysed sites, the OH formed from vCIs more influenced to the formation of $\text{SO}_4^{2-}(\text{p})$ than sCIs, but in the remote sites, their difference became closer. Compared with the unimolecular reaction of sCIs and the reaction of sCIs with water, water was more relevant to the sCI-loss reactions at all analysed sites. The loss of sCIs by HNO_3 and organic acids is as important as the loss by unimolecular decomposition and water. In terms of the comparison of vCIs and sCIs with $\text{SO}_4^{2-}(\text{p})$ formation, this is the first study to clarify the quantitative relationship between them in highly industrialised and rural/remote sites, concluding that sCI-chemistry should be considered in rural and remote areas.

Uncertainties of this work



Although several impacts of Cls on $\text{SO}_4^{2-}(\text{p})$ formation were updated in this study, the uncertainties of the analysis must be addressed. There are two types of uncertainties in the analyses: those associated with the CTM itself and those related to the chemical reactions incorporated in this study. Regarding the uncertainties of the CTM, several factors contribute, including emission inventories, meteorological parameters, gas-phase, heterogeneous, and aqueous-phase chemistries incorporated in the default CTM. The combinations of these uncertainties ultimately resulted in the outcomes shown in Fig. 2, which indicate a correlation between the observed and modelled results for the column density of O_3 , HCHO , and SO_2 , although the replicability is not perfect. As discussed above, the discrepancies may stem from the differences in grid resolution between the observed and calculated results, as well as the accumulation of errors in the vertical layer summation process calculated by the CTM. There is also a possibility of inaccuracies in the emission inventories. Nevertheless, we must accept the errors caused by the CTM itself, as all current CTMs have inherent uncertainties. It is important to note that the results obtained in this study should be treated as one of the conclusions with potential errors stemming from the CTM. The uncertainties arising from the incorporated reactions of Cls should be treated more carefully, as the inclusion of Cl-chemistry is the main focus of this study. The results in Fig. 5 suggest that considering only 30% of NO_3 formation by sCl + NO_2 reactions leads to NO_2 removal,⁴⁵ thus contributing to a reduction in tropospheric NO_3 , a phenomenon opposite to that observed in previous work.¹⁸ Furthermore, the sensitivity analyses shown in Figs. 6–8 indicate that the sensitivities of other Cl-related chemical reactions are higher than that of the sCl + NO_2 reactions. This suggests that the definition and accuracy of the chemical mechanisms applied in the CTM affect the atmospheric impacts induced by Cl-chemistry. For example, Sarwer et al. conducted CTM calculations by adding the chemical mechanisms of sCl for both low- and high-rate constants of sCl + water reactions to clarify the potential influence of uncertainties in these reactions.⁵⁰ The results suggested that the contribution of sCl to $\text{SO}_4^{2-}(\text{p})$ was more than an order of magnitude higher when lower rate constants for sCl + water reactions were applied. Lade et al. conducted experimental and theoretical approaches to determine the rate constant of SCI1 (formaldehyde oxide) and water reactions, as well as CTM calculations to assess the atmospheric impact of the water monomer and dimer.⁵¹ They concluded that more than 98% of SCI1 is consumed by the water dimer, but the uncertainties in the product yields of SCI1 + water reactions limit the understanding of SCI1 chemistry. In terms of the rate constants for the unimolecular decomposition of sCl, this study used the values obtained by Vereecken et al.,²⁰ which were estimated based on classical TST calculations coupled with the semi-empirical method and structure–activity relationships. However, the experimental and theoretical studies for the determination of the rate constant for the unimolecular decomposition of dimethyl-substituted Cls, conducted by Lester and Klippenstein, suggested the importance of applying high-pressure limit calculations (master equation method) to

determine the rate constant under ambient conditions and of adjusting tunnelling parameters.⁵² The rate constant estimated by Vereecken et al. was reported to be approximately 1.5 times higher than that of Lester and Klippenstein. The branching ratios of the reaction mechanisms of Cl-chemistry incorporated in this study also hold several uncertainties, as the products of nearly all reactions involve assumptions due to a lack of information (e.g. assuming 0.5 for the branching ratio of *E*- and *Z*-isomers of sCl after alkene ozonolysis, assuming complete dissociation of unimolecular decay to form OH, assuming the same rate constants for all sCl + HNO_3 reactions, etc.). Despite these uncertainties, one of the main topics of this study is to clarify the importance of vCl-initiated OH formation in $\text{SO}_4^{2-}(\text{p})$ formation. According to the results in Figs. 6–8, the sensitivities of the reaction kinetics of vCl and sCl on $\text{SO}_4^{2-}(\text{p})$ formation are an order of magnitude higher than those of the sCl-loss reactions. For these reasons, although several reaction mechanisms incorporated in this study involve uncertainties, the contribution of vCl remains plausible. Further studies should be conducted to clarify the uncertainties in reaction kinetics, branching ratios, and other aspects of Cl-chemistry in future work.

Summary

The impact of chemical reactions related to Cls on $\text{SO}_4^{2-}(\text{p})$ and other aerosol species was evaluated using a global CTM. The absolute amount of $\text{SO}_4^{2-}(\text{p})$ formation was high in China and India because of high SO_2 pollution, while the percentage of the contribution of Criegee-chemistry was maximally approximately 0.5% in the Amazon rainforests. The most relevant sCl on a global scale estimated in this study was ESCI7, the *E*-isomer of the sCl formed by the ozonolysis of MVK, owing to the relatively low rate of atmospheric loss processes, which indicates the necessity for further kinetic studies related to ESCI7 chemistry. The results of the sensitivity analyses suggested that in all analysed sites, the OH formed by the unimolecular decomposition of vCl can influence more to $\text{SO}_4^{2-}(\text{p})$ formation than the direct oxidation of SO_2 by sCl, especially in industrialised areas. This indicates that, in terms of aerosol formation via Criegee chemistry, the unimolecular decomposition of vCl is more important in aerosol formation, and sCl increase its importance in the remote area. The sCl loss reactions involving HNO_3 and organic acids are as important for $\text{SO}_4^{2-}(\text{p})$ formation as those involving the unimolecular decomposition of sCl and water.

The results of this study showcase the overall global impact of Cls on the formation of tropospheric $\text{SO}_4^{2-}(\text{p})$ and related aerosol species, but there are several assumptions for the rate constants set in this study (e.g., temperature dependence was not considered for the reactions of sCl with SO_2 , NO_2 , etc., and the branching ratio of *E*- and *Z*-isomers was set to 0.5) because of the limited information available on the gas-phase kinetics of sCl. Further kinetic studies on sCl should be conducted in the future works. Furthermore, several studies have revealed the heterogeneous kinetics between the gas/liquid interface of Cls reacting with H_2O , alcohol, etc., forming hydroxy hydroperoxide



(HHP), alkoxy alkyl hydroperoxide (AAHP), liquid-phase OH, and RO₂, which are important oxidisers in the liquid phase that contribute to the formation of particulate matter.⁵³⁻⁵⁵ Besides the detailed gas-phase chemistry of CI, the heterogeneous kinetics of CI should be evaluated by chemical transport modelling in future work to detail the effect of CI on the atmosphere.

Author Contributions

Hiroo Hata proposed the research concept, conducted global chemical transport modelling, and wrote the draft paper. Yuya Nakamura determined the kinetic parameters of the Criegee intermediates and checked the paper for accuracy. Jairo Vazquez Santiago analysed satellite data obtained from TROPOMI and checked the paper for accuracy. Kenichi Tonokura supervised and checked the work for accuracy.

Conflicts of interest

There are no conflicts to declare.

Acknowledgements

This study was supported by a Grant-in-Aid for Scientific Research (B) from the Japan Society for the Promotion of Science (JSPS; Grant Number JP24K03088).

References

- Pope III, A.C.; Burnett, T.R.; Thun, J.M. Lung cancer, cardiopulmonary mortality, and long-term exposure to fine particulate air pollution. *JAMA*. 2002, 287(9), 1132-1141.
- Kim, K.-H.; Kabir, E.; Kabir, S. A review on the human health impact of airborne particulate matter. *Environ. Int.* 2015, 74, 136-143.
- Burnett, R.; Chen, H.; Szyszkwicz, M.; Spadaro, V.J. Global estimates of mortality associated with long-term exposure to outdoor fine particulate matter. *Proc. Natl. Acad. Sci. U.S.A.* 2018, 115(38), 9592-9597.
- Zhang, R.; Wang, G.; Guo, S.; Zamora, L.M.; Ying, Q.; Lin, Y.; Wang, W.; Hu, M.; Wang, Y. Formation of urban fine particulate matter. *Chem. Rev.* 2015, 115(10), 3803-3855.
- Singh, S.; Soni, K.; Bano, T.; Tanwar, S.R.; Nath, S.; Arya, C.B. Clear-sky direct aerosol radiative forcing variations over mega-city Delhi. *Ann. Geophys.* 2010, 28, 1157-1166.
- Wang, Q.; Jacob, J.D.; Fisher, A.J.; Mao, J.; Leibensperger, M.E.; Carouge, C.C.; Sager, Le, P.; Kondo, Y.; Jimenez, L.J.; Cubison, J.M.; Doherty, J.S. Sources of carbonaceous aerosols and deposited black carbon in the Arctic in winter-spring: implications for radiative forcing. *Atmos. Chem. Phys.* 2011, 11, 12453-12473.
- Hassan, Z.; Stahlberger, M.; Rosenbaum, N.; Bräse, S. Criegee intermediates beyond ozonolysis: synthetic and mechanistic insights. *Angew. Chem. Int. Ed.* 2021, 60, 15138-15152.
- Taatjes, A.C.; Shallcross, E.D.; Percival, J.C. Research frontiers in the chemistry of Criegee intermediates and tropospheric ozonolysis. *Phys. Chem. Chem. Phys.* 2014, 16, 1704-1718.
- Chhantyal-Pun, R.; Khan, H.A.M.; Taatjes, A.C.; Percival, J.C. Criegee intermediates: production, detection and reactivity. *Int. Rev. Phys. Chem.* 2020, 39(3), 385-424.
- Khan, H.A.M.; Percival, J.C.; Caravan, L.R.; Taatjes, A.C.; Shallcross, E.D. Criegee intermediates and their impacts on the troposphere. *Environ. Sci.: Processes Impacts* 2018, 20, 437-453.
- Osborn, L.D.; Taatjes, A.C. The physical chemistry of Criegee intermediates in the gas phase. *Int. Rev. Phys. Chem.* 2015, 34(3), 309-360.
- Lester, I.M.; Klippenstein, J.S. Unimolecular decay of Criegee intermediates to OH radical product: prompt and thermal decay processes. *Acc. Chem. Res.* 2018, 51(4), 978-985.
- Kidwell, M.N.; Li, H.; Wang, X.; Bowman, M.J.; Lester, I.M. Unimolecular dissociation dynamics of vibrationally activated CH₃CHO Criegee intermediates to OH radical products. *Nat. Chem.* 2016, 8, 509-514.
- Sarwer, G.; Simon, H.; Fahey, K.; Mathur, R.; Goliff, S.W.; Stockwell, R.W. Impact of sulfur dioxide oxidation by Stabilized Criegee Intermediate on sulfate. *Atmos. Environ.* 2014, 85, 204-214.
- Percival, J.C.; Welz, O.; Eskola, J.A.; Savee, D.J.; Osborn, L.D.; Topping, O.D.; Lowe, D.; Utembe, R.S.; Bacak, A.; McFiggans, G.; Cooke, C.M.; Xiao, P.; Archibald, T.A.; Jenkin, E.M.; Derwent, G.R.; Riipinen, I.; Mok, K.W.D.; Lee, F.P.E.; Dyke, M.J.; Taatjes, A.C.; Shallcross, E.D. Regional and global impacts of Criegee intermediates on atmospheric sulphuric acid concentrations and first steps of aerosol formation. *Faraday Discuss.* 2013, 165, 45-73.
- Nakamura, Y.; Hata, H.; Tonokura, K. Urban-scale analysis of the seasonal trend of stabilized-Criegee intermediates and their effect on sulphate formation in the Greater Tokyo Area. *Environ. Sci.: Atmos.* 2023, 3, 1758-1766.
- Cox, A.R.; Ammann, M.; Crowley, N.J.; Herrmann, H.; Jenkin, E.M.; McNeill, F.V.; Mellouki, A.; Troe, J.; Wallington, J.T. Evaluated kinetic and photochemical data for atmospheric chemistry: Volume VII – Criegee intermediates. *Atmos. Chem. Phys.* 2020, 20(21), 13497-13519.
- Hata, H.; Hoshino, S.; Fujita, M.; Tonokura, K. Atmospheric impact of isoprene-derived Criegee intermediates and isoprene hydroxy hydroperoxide on sulfate aerosol formation in the Asian region. *Atmos. Environ.: X* 2023, 20, 100226.
- Newland, J.M.; Rickard, R.A.; Vereecken, L.; Muñoz, A.; Ródenas, M.; Bloss, J.W. Atmospheric isoprene ozonolysis: impacts of stabilised Criegee intermediate reactions with SO₂, H₂O and dimethyl sulfide. *Atmos. Chem. Phys.* 2015, 15, 9251-9256.
- Vereecken, L.; Novelli, A.; Taraborrelli, D. Unimolecular decay strongly limits the atmospheric impact of Criegee intermediates. *Phys. Chem. Chem. Phys.* 2017, 19, 31599-31612.
- Sheps, L.; Rotavera, B.; Eskola, J.A.; Osborn, L.D.; Taatjes, A.C.; Au, K.; Shallcross, E.D.; Khan, H.A.M.; Percival, J.C. The reaction of Criegee intermediate CH₂OO with water dimer: primary products and atmospheric impact. *Phys. Chem. Chem. Phys.* 2017, 19, 21970-21979.
- McGillen, R.M.; Curchod, E.F.B.; Chhantyal-Pun, R.; Beames, M.J.; Watson, N.; Khan, H.A.M.; McMahon, L.; Shallcross, E.D.; Orr-Ewing, J.A. Criegee intermediate-alcohol reactions, a potential source of functionalized hydroperoxides in the atmosphere. *ACS Earth Space Chem.* 2017, 1(10), 664-672.
- Caravan, L.R.; Vansco, F.M.; Au, K.; Lester, I.M. Direct kinetic measurements and theoretical predictions of an isoprene-derived Criegee intermediate. *Proc. Natl. Acad. Sci. U.S.A.* 2020, 117(18), 9733-9740.
- Newland, J.M.; Rickard, R.A.; Sherwen, T.; Evans, J.M.; Vereecken, L.; Muñoz, A.; Ródenas, M.; Bloss, J.W. The atmospheric impacts of monoterpene ozonolysis on global stabilised Criegee intermediate budgets and SO₂ oxidation: experiment, theory and modelling. *Atmos. Chem. Phys.* 2018, 18, 6095-6120.



- 25 Chhantyal-Pun, R.; Khan, H.A.M.; Zachhuber, N.; Percival, J.C.; Shallcross, E.D.; Orr-Ewing, J.A. Impact of Criegee intermediate reactions with peroxy radicals on tropospheric organic aerosol. *ACS Earth Space Chem.* 2020, 4(10), 1743-1755.
- 26 GEOS-Chem v14.2.3. 10.5281/zenodo.10246625.
- 27 Gelaro, R.; McCarty, W.; Suárez, M.J.; Todling, R.; Molod, A.; Takacs, L.; Randles, C.A.; Darmenov, A.; Bosilovich, M.G.; Reichle, R.; Wargan, K.; Coy, L.; Cullather, R.; Draper, C.; Akella, S.; Buchard, V.; Conaty, A.; da Silva, A.M.; Gu, W.; Kim, G.-K.; Koster, R.; Lucchesi, R.; Merkova, D.; Nielsen, J.E.; Partyka, G.; Pawson, S.; Putman, W.; Rienecker, M.; Schubert, S.D.; Sienkiewicz, M.; Zhao, B. Modern era retrospective analysis for research and applications version 2 (MERRA-2). *J. Clim.* 2017, 30(14), 5419-5454.
- 28 Lin, H.; Jacob, J. D.; Lundgren, W. E.; Sulprizio, P. M.; Keller, A. C.; Fritz, M. T.; Eastham, D. S.; Emmons, K. L.; Campbell, C. P.; Baker, B.; Saylor, D. R.; Montuoro, R. Harmonized emissions component (HEMCO) 3.0 as a versatile emissions component for atmospheric models: application in the GEOS-Chem, NASA GEOS, WRF-GC, CESM2, NOAA GEFS-Aerosol, and NOAA UFS models. *Geosci. Model Dev.* 2021, 14, 5487-5506.
- 29 McDuffie, E.E.; Smith, S.J.; O'Rourke, P.; Tibrewal, K.; Venkataraman, C.; Marais, E.A.; Zheng, B.; Crippa, M.; Brauer, M.; Martin, R.V. A global anthropogenic emission inventory of atmospheric pollutants from sector- and fuel-specific sources (1970-2017): an application of the Community Emissions Data System (CEDS). *Earth Syst. Sci. Data* 2020, 12, 3413-3442.
- 30 Janssens-Maenhout, G.; Crippa, M.; Guizzardi, D.; Dentener, F.; Muntean, M.; Pouliot, G.; Keating, T.; Zhang, Q.; Kurokawa, J.; Wankmüller, R.; Denier van der Gon, H.; Kuenen, J.J.P.; Klimont, Z.; Frost, G.; Darras, S.; Koffi, B.; Li, M. HTAP_v2.2: A mosaic of regional and global emission grid maps for 2008 and 2010 to study the hemispheric transport of air pollution. *Atmos. Chem. Phys.* 2015, 15, 11411-11432.
- 31 Pham, V.V.; Tang, J.; Alam, S.; Lokan, C.; Abbass, H.A. Aviation emission inventory development and analysis. *Environ. Modell. Softw.* 2010, 25(12), 1738-1753.
- 32 van der Werf, G.R.; Randerson, J.T.; Giglio, L.; van Leeuwen, T.T.; Chen, Y.; Rogers, B.M.; Mu, M.; van Marle, M.J.E.; Morton, D.C.; Collatz, G.J.; Yokelson, R.J.; Kasibhatla, P.S. Global fire emissions estimates during 1997-2016. *Earth Syst. Sci. Data* 2017, 9(2), 697-720.
- 33 Dentener, F.; Kinne, S.; Bond, T.; Boucher, O.; Cofala, J.; Generoso, S.; Ginoux, P.; Gong, S.; Hoelzemann, J.J.; Ito, A.; Marelli, L.; Penner, J.E.; Putaud, J.-P.; Textor, C.; Schulz, M.; van der Werf, G.R.; Wilson, J. Emissions of primary aerosol and precursor gases in the years 2000 and 1750 prescribed datasets for AeroCom. *Atmos. Chem. Phys.* 2006, 6, 4321-4344.
- 34 Guenther, A.B.; Jiang, X.; Heald, C.L.; Sakulyanontvittaya, T.; Duhl, T.; Emmons, L.K.; Wang, X. The Model of Emissions of Gases and Aerosols from Nature version 2.1 (MEGAN2.1): an extended and updated framework for modeling biogenic emissions. *Geosci. Model Dev.* 2012, 5, 1471-1492.
- 35 Garane, K.; Koukouli, M.-E.; Lerot, C.V.T.; Heue, K.-P.; Fioletov, V.; Balis, D.; Bais, A.; Bazureau, A.; Dehn, A.; Goutail, F.; Granville, J.; Griffin, D.; Hubert, D.; Keppens, A.; Lambert, J.-C.; Loyola, D.; McLinden, C.; Pazmino, A.; Pommereau, J.-P.; Redondas, A.; Romahn, F.; Valks, P.; Van Roozendaal, M.; Xu, J.; Zehner, C.; Zerefos, C.; Zimmer, W. TROPOMI/S5P total ozone column data: global ground-based validation and consistency with other satellite missions. *Atmos. Meas. Tech.* 2019, 12, 5263-5287.
- 36 van Geffen, J.; Boersma, F.K.; Eskes, H.; Sneep, M.; ter Linden, M.; Zara, M.; Veefkind, P.J. S5P TROPOMI NO₂ slant column retrieval: method, stability, uncertainties and comparisons with OMI. *Atmos. Meas. Tech.* 2020, 13(3), 1315-1335.
- 37 Vigouroux, C.; Langerock, B.; Aquino, B.A.C.; Blumenstock, T.; Cheng, Z.; De Mazière, M.; De Smedt, I.; Grutter, M.; Hannigan, W.J.; Jones, N.; Kivi, R.; Loyola, D.; Lutsch, E.; Mahieu, E.; Makarova, M.; Metzger, J.-M.; Morino, I.; Murata, I.; Nagahama, T.; Notholt, J.; Ortega, I.; Palm, M.; Pinardi, G.; Röhling, A.; Smale, D.; Stremme, W.; Strong, K.; Sussmann, R.; Té, Y.; van Roozendaal, M.; Wang, P.; Winkler, H. TROPOMI-Sentinel-5 Precursor formaldehyde validation using an extensive network of ground-based Fourier-transform infrared stations. *Atmos. Meas. Tech.* 2020, 13(7), 3751-3767.
- 38 Hong, Q.; Liu, C.; Hu, Q.; Zhang, Y.; Xing, C.; Su, W.; Ji, X.; Xiao, S. Evaluating the feasibility of formaldehyde derived from hyperspectral remote sensing as a proxy for volatile organic compounds. *Atmos. Res.* 2021, 264, 105777.
- 39 Data archive of COPERNICUS. <https://sentinels.copernicus.eu/web/sentinel/home> (accessed June 4, 2024).
- 40 NASA EarthData archive. <https://www.earthdata.nasa.gov/> (accessed June 4, 2024).
- 41 Murphy, B.N.; Nolt, G.C.; Sidi, F.; Bash, O.J.; Appel, W.K.; Jang, C.; Kang, D.; Kelly, J.; Mathur, R.; Napelenok, S.; Pouliot, G.; Pye, T.O.H. The detailed emissions scaling, isolation, and diagnostic (DESID) module in the community multiscale air quality (CMAQ) modeling system version 5.3.2. *Geosci. Model Dev.* 2021, 14, 3407-3420.
- 42 Carter, W.P.L. Development of the SAPRC-07 chemical mechanism. *Atmos. Environ.* 2010, 44(40), 5324-5335.
- 43 Saunders, M.S.; Jenkin, E.M.; Derwent, G.R.; Pilling, J.M. Protocol for the development of the Master Chemical Mechanism, MCM v3 (Part A): tropospheric degradation of non-aromatic volatile organic compounds. *Atmos. Chem. Phys.* 2003, 3, 161-180.
- 44 Smith, C.M.; Chang, C.-H.; Chao, W.; Lin, L.-C.; Takahashi, K.; Boering, A.K.; Jr-Min Lin, J. Strong negative temperature dependence of the simplest Criegee intermediate CH₂OO reaction with water dimer. *J. Phys. Chem. Lett.* 2015, 6(14), 2708-2713.
- 45 Caravan, L.R.; Khan, H.A.M.; Rotavera, F.; Papajak, E.; Antonov, O.I.; Chen, M.-W.; Au, K.; Chao, W.; Osborn, L.D.; Jr-Min Lin, J.; Percival, J.C.; Shallcross, E.D.; Taatjes, A.C. Products of Criegee intermediate reactions with NO₂: experimental measurements and tropospheric implications. *Faraday Discuss.* 2017, 200, 313-330.
- 46 Huang, H.-L.; Chao, W.; Lin Jr. M.J. Kinetics of a Criegee intermediate that would survive high humidity and may oxidize atmospheric SO₂. *Proc. Natl. Acad. Sc. U.S.A.* 2015, 112, 10857-10862.
- 47 Fountoukis, C.; Nenes, A. ISORROPIA II: a computationally efficient thermodynamic equilibrium model for K⁺-Ca²⁺-Mg²⁺-NH⁴⁺-Na⁺-SO₄²⁻-NO₃⁻-Cl⁻-H₂O aerosols. *Atmos. Chem. Phys.* 2007, 7, 4639-4659.
- 48 Budisulistiorini, S.H.; Nenes, A.; Cariton, A.G.; Surratt, J.D.; McNeill, V.F.; Pye, H.O.T. Simulating aqueous-phase isoprene epoxydiol (IEPOX) secondary organic aerosol production during the 2013 Southern Oxidant and Aerosol Study (SOAS). *Environ. Sci. Technol.* 2017, 51(9), 5026-5034.
- 49 Ng, L.N.; Brown, S.S.; Archibald, T.A.; Atlas, E.; Cohen, C.R.; Crowley, N.J.; Day, A.D.; Donahue, M.N.; Fry, L.J.; Fuchs, H.; Griffin, J.R.; Guzman, I.M.; Herrmann, H.; Hodzic, A.; Iinuma, Y.; Jimenez, L.J.; Kiendler-Scharr, A.; Lee, H.B.; Luecken, J.D.; Mao, J.; McLaren, R.; Mutzel, A.; Osthoff, D.H.; Ouyang, B.; Picquet-Varrault, B.; Platt, U.; Pye, T.O.H.; Yinon Rudich, Y.; Schwantes, H.R.; Shiraiwa, M.; Stutz, J.; Thornton, A.J.; Tilgner, A.; Williams, J.B.; Zaveri, A.R. Nitrate radicals and biogenic volatile organic compounds: oxidation, mechanisms, and organic aerosol. *Atmos. Chem. Phys.* 2017, 17, 2103-2162.
- 50 Sarwar, G.; Fahey, K.; Kwok, R.; Gilliam, R.C.; Roselle, J.S.; Mathur, R.; Xue, J.; Yu, J.; Carter, W.P.L. Potential impacts of



ARTICLE

Journal Name

- two SO₂ oxidation pathways on regional sulfate concentrations: Aqueous-phase oxidation by NO₂ and gas-phase oxidation by Stabilized Criegee Intermediates. *Atmos. Environ.* 2013, 68, 186-197.
- 51 Lade, R.E.; Blitz, M.A.; Rowlinson, M.; Evans, M.J.; Seakins, P.W.; Stone, D. Kinetics of the reactions of the Criegee intermediate CH₂OO with water vapour: experimental measurements as a function of temperature and global atmospheric modelling. *Environ. Sci.: Atmos.* 2024, 4, 1294-1308.
- 52 Lester, M.I.; Klippenstein, S.J. Unimolecular decay of Criegee intermediates to OH radical products: prompt and thermal decay processes. *Acc. Chem. Res.* 2018, 51(4), 978-985.
- 53 Qiu, J.; Ishizuka, S.; Tonokura, K.; Colussi, J.A.; Enami, S. Reactivity of monoterpene Criegee intermediates at gas-liquid interfaces. *J. Phys. Chem. A* 2018, 122(39), 7910-7917.
- 54 Zeng, M.; Wilson, R.K. Efficient coupling of reaction pathways of Criegee intermediates and free radicals in the heterogeneous ozonolysis of alkenes. *J. Phys. Chem. Lett.* 2020, 11(16), 6580-6585.
- 55 Zhao, Z.; Xu, Q.; Yang, X.; Zhang, H. Heterogeneous ozonolysis of endocyclic unsaturated organic aerosol proxies: implications for Criegee intermediate dynamics and later-generation reactions. *ACS Earth Space Chem.* 2019, 3(3), 344-356.

View Article Online
DOI: 10.1039/D4EA00137K



View Article Online
DOI: 10.1039/D4EA00137K

The data supporting this article are included as part of the main text and in the ESI.

